Management options influence seasonal CO_2 soil emissions in Mediterranean olive ecosystems

Giuseppe Montanaro[1*], Georgios Doupis[2], Nektarios Kourgialas[2], Emmanouel Markakis[2], Nektarios Kavroulakis[2], Georgios Psarras[2], Georgios Koubouris[2], Bartolomeo Dichio[1], Vitale Nuzzo[1]

[1]Università degli Studi della Basilicata – Via N. Sauro, 85100 Potenza - (Italy)

[2] ELGO-DIMITRA, Institute of Olive Tree, Subtropical Crops and Viticulture, Leoforos Karamanli 167, Chania GR-73134, Greece

*Corresponding author

E-mail: giuseppe.montanaro@unibas.it Phone +39 391 3808337

ORCID 0000-0002-1172-7526

Address:

Università degli Studi della Basilicata – Via N. Sauro, 85 – 85100 Potenza, Italy

Abstract

Field trials were conducted at traditional Mediterranean olive agro-ecosystems grown at two locations (Italy –IT, Greece –GR). Groves were managed for many years using sustainable (*S*, cover crops, compost application, mulching of pruning biomass) or conventional (*C*) practices (e.g., soil tillage, burning of pruning residuals). The IT grove was rainfed ($_{RAIN}$) while the GR was irrigated ($_{IRR}$). This study examined the seasonal variation of soil CO_2 emission (R_s) to explore the effect of the management options (*C*, *S*) on R_s at both sites. The second aim was to test the hypothesis that the seasonal R_s is differentially modulated by soil temperature and moisture, namely that (*i*) soil moisture limits R_s when it is below the lower limit of the readily available water (RAW_{LLim}) and (*ii*) soil temperature above a threshold (max_T) reduces R_s even if soil moisture is non limiting. On the whole-season basis, the mean R_s rate at the rainfed site was 2.17±0.06 (SE) at C_{RAIN} and 2.32±0.06 μmol CO_2 m^{-2} s^{-1} at S_{RAIN} plot, while at the irrigated site R_s was about 3.64±0.11 (C_{IRR}) and 4.05±0.15 μmol CO_2 m^{-2} s^{-1} (S_{IRR}). The seasonal oscillation of R_s was consistent across locations and partitionable in three periods according to DOY (Day of Year) interval: Phase I (DOY 20-103 –GR; 20-118 -IT), Phase II (DOY 141÷257, GR; 142-257, IT) and Phase III (DOY 291-357, GR; 286-350, -IT). Pooling all the R_s data across sites and managements, max_T was ~ 20°C discriminating a differential response of R_s when soil moisture was < or > RAW_{LLim}. These differential modulations exerted by temperature and moisture were integrated into a conditional model developed with a repeated random subsampling cross-validation procedure to effectively (R^2 = 0.84) predict R_s. This paper mechanistically describes the interaction of the environment (soil moisture and temperature) and the management options (*S*, *C*) under various moisture conditions on

R_s and would support carbon flux accounting procedures (e.g., regulating ecosystem services) tailored to the estimation of sink/source capability of traditional olive agro-ecosystem within environmental-friendly agricultural domains.

Key words: carbon cycle; conditional model; irrigation; rainfed; soil moisture; soil organic carbon; soil respiration; soil temperature; sustainable; traditional system.

1. Introduction

The potential contribution of agricultural ecosystems to climate change mitigation is actively debated, considering both increasing carbon (C) sequestration and reducing greenhouse gas (GHG) emissions (Sanz-Cobena et al., 2017). Cropland has been recognized among land use types (e.g., forestry land, grassland, wetlands) that influence a variety of ecosystem processes and, in turn, ecosystem services related to GHG fluxes (e.g., photosynthesis, soil respiration, decomposition) (Eggleston et al, 2006, Montanaro et al., 2017a).

The global carbon cycle includes CO_2 uptake from the atmosphere through photosynthesis (Gross Primary Productivity, GPP); the imbalance between GPP and the CO_2 loss by autothrophic respiration is the Net Ecosystem Productivity (NPP). The carbon cycle also includes soil CO_2 emissions (soil respiration, R_s), which account for about 85–90% of the GPP and about 55-77% of the NPP (Xu and Shang, 2016; Montanaro et al., 2017b), confirming that R_s is pivotal for ecosystem carbon budget.

The agricultural sector currently pursues the restoration of the soil C reservoir through more sustainable soil management practices aimed at increasing soil C input and minimising CO_2 emissions, compared to conventional. Increased C inputs boost soil fertility by raising soil organic C content which, in turn, enhances a number of soil nutritional and functional proprieties (e.g. soil water infiltration rate and retention, soil porosity and stability) (Bhogal et al., 2009, Montanaro et al., 2018). However, increasing C input to the soil is expected to increase R_s (Franzluebbers et al., 2002, Wang et al., 2003).

The rate of R_s is affected by several factors and their interaction. Xu and Shang (2016) reviewed these factors, highlighting the primary influence of climate (e.g., soil temperature and moisture), vegetation (e.g., litter and biomass production, root exudation), and soil features (e.g., C concentration, structure). Within cultivated ecosystems, some of these factors are manageable by the grower and useful for sustainable recarbonization purposes due to their influence on the overall C budget, including R_s. For example, the adoption of cover crops, *in loco* mulching of pruning residuals, and the addition of external organic fertilizers (e.g., compost, manure) might impact the content of soil organic carbon (SOC) (Aguillera et al., 2013; Koubouris et al., 2017; Montanaro et al., 2017; Kavvadias et al., 2018; Kavvadias and Koubouris, 2019; Michalopoulos et al., 2020; Plénet et al. 2022).

About 90% of the global olive plantations are located in Mediterranean countries (FAO, 2022) which are almost entirely under traditional plantation systems (up to 300 trees per ha) (Rallo et al., 2014; FAO, 2022). At these plantations, irrigation has also been introduced (Rallo et al., 2014), likely increasing substrate availability and accelerating the oxidation of C substrates by microorganisms as per the combination with high soil temperatures (Fang and Moncrieff, 2001). Hence, an increased soil CO_2 flux in sustainable (e.g., high C input) traditional irrigated groves is expected compared to conventional. In addition, due to seasonal variations in soil moisture under Mediterranean conditions (Kourgialas et al., 2017; Arampatzis et al., 2018), sesonal oscillations of R_s would also be expected. However, detailed data on seasonal variation of R_s as influenced by management practices (e.g., carbon retention) under irrigation or rainfed are still limited. Therefore, the first aim of the present paper was to examine the seasonal variability of R_s as influenced by soil recarbonization management practices under rainfed and irrigation.

Soil temperature is a dominant environmental driver of R_s and their relationship is usually depicted by exponential equations (Subke et al., 2003). However, when the temperature is above a threshold value, the R_s declines because of co-occurring constraints (e.g., SOC, microbial biomass) also under non-limiting moisture (Richardson et al., 2012, Carey et al., 2016). Soil moisture influence R_s also indirectly because values below the lower limit of the readiliy available water (RAW_{LLim}) lowers leaf water potential and in turn plant photosynthesis which modulate the autotrophic component of R_s (Tang et al., 2005, Hernández-Montes et al., 2017).

Variation of soil moisture and temperature would influence their impact on R_s hampering a clear identification of the prominent factor limiting or promoting R_s. In order to improve the predictability of R_s, Almagro et al., (2009) proposed a month-based partition of the season into “growing” (October-April) and “dry” (May-September) seasons. However, a mechanistic modeling of the main limiting/promoting factors of R_s based on (easily accessible) environmental variables would be desirable. Additional knowledge of the influence of management options and the environment (soil temperature and moisture) on R_s at traditional olive plantations would strengthen the assessment of the regulating ecosystem services based on C balance.

Hence, the second aim of this study was to test the hypothesis that soil temperature and moisture differentially modulate the seasonal R_s based on their threshold values, namely that (*i*) soil moisture becomes a limiting factor of R_s at the level below RAW_{LLim} and that (*ii*) temperature above a maximum (max_T) threshold reduces R_s, even if soil moisture lies within RAW. The threhold values and the fitting model of predictors (soil moisture and temperature) were then combined in a conditional model to predict the response variables (R_s).

2. Materials and methods

2.1 Experimental sites and treatments imposition

In this study, the imposed factor was the "management" at two levels: Sustainable (S) and Conventional (C). The S treatment was a set of practices achieving a higher retention of carbon in the agro-ecosystem compared to that of the C one. Soil moisture and temperature and soil CO_2 emission (R_s) were the covariates measured upon management treatment imposition. The R_s was then modelled as response variable based on changes in soil moisture and temperature. The experiment was carried out in open fields located in Italy and Greece, differing in water supply: rainfed (Italy, suffix $_{RAIN}$) and irrigation (Greece, $_{IRR}$). The Italian and Greek experimental sites were representative of the olive groves of the studied areas, further details are specifically reported in the following sections.

2.1.1 Rainfed Italian site

The Italian olive grove was located at a private farm (Matera province, 40° 29' N, 16° 27' E) on a hilly area (16% slope) and was rainfed ($_{RAIN}$). The locally conventional practices

(C_{RAIN}), the soil was tilled (10-15 cm depth) 2-3 times a year during the growing season, pruning was done in winter, and all residues were removed and burnt; nitrogen was evenly distributed on the soil (centrifugal fertilizer spreader) at a mean rate of approx. 40 kg ha^{-1}. From 2000, an approx. 0.7 ha block was subjected to sustainable management (S_{RAIN}) where the soil was untilled and the understorey 'grass' was mowed two times a year to 3-4 cm. Fertilization was designed to fill the gap between tree demand and the availability of essential nutrients in the soil (Montanaro et al., 2010). Pruning was done each year in December and January and the pruning biomass was chipped and evenly distributed in the alley at a mean rate of about 1.12 t C ha^{-1} estimated according to Palese et al., (2013). On average (0-0.5 m depth) at the C_{RAIN} plot, the soil was sandy-loam (64.7% sand, 21.0% silt, and 15.0% clay) and had pH 7.9, OM 1.29%. At the S_{RAIN}, soil texture had pH 7.6, 66.2% sand, 17.9% silt, 15.7% clay, OM 1.67%. Then, the lower limit of the readily available water (RAW_{LLim}) of 11.1 %dw (C_{RAIN}) and 11.4%dw (S_{RAIN}) were calculated assuming 1.3 t m^{-3} BD according to Saxton and Rawl (2006). The site was 365 m a.s.l.. The trees (*Olea europaea* L., cv Maiatica) were >50-year old and spaced at 8 × 8 m (156 p ha^{-1}). The long-term (1981-2018) average annual rainfall in the region is about 523 mm and is highly seasonal, usually falling between October and May, with insignificant amounts between June and September. The average maximum annual air temperature is 31.8°C (SAL Service, ALSIA Basilicata Region). At the harvest time, the yield of 8 trees per treatment was measured (FW), averaged and reported as t ha^{-1}.

2.1.2 Irrigated Greek site

In Greece, the study was performed at a 40-year-old olive plantation (1.1 ha) located in the experimental station of the Institute of Olive Tree, Subtropical Crops and Viticulture, Nerokourou, Crete island, Southern Greece (35°28′36.76″N, 24°02′36.44″ E; 51 m a.s.l). Trees (*Olea europaea* L., cv. Kalamon) were planted at 7 × 7 m. According to the local meteorological station, the average maximum annual air temperature was 33.0 °C, the air relative humidity was 64%, and the annual rainfall was 700 mm. The olive grove was weekly irrigated (suffix $_{IRR}$) from May to September, according to the reference evapotranspiration retrieved by the local weather station and crop coefficients (Kourgialas et al., 2019). Each row had an irrigation line with five drippers per tree (4 L h^{-1} discharge rate per dripper), wetting a ∼1.0 m wide soil band along the row.

From 2011, a sustainable treatment (S_{IRR}) was imposed through a completely randomized design, with three replicates (*n* = 3) for a total of 12 trees (4 olive trees per plot). The S_{IRR} employed the application of commercial compost. The compost was obtained from recycled olive mill by-products (olive leaves, fruit pulps and stones, and liquid waste) and was evenly distributed (centrifugal fertilizer spreader) to the soil surface between February-March each year. The annual amount (fresh weight) of compost distributed in a single time was 6 t ha^{-1} (2013) and 9 t ha^{-1} (2014, 2015). The compost had the following characteristics: C/N = 18, pH 7.8; 49.76% total C (w/w, on dry matter basis), 2.77% (w/w) total N, 2.26% (w/w) total K, and 0.18% (w/w) total P. The S_{IRR} also received the pruning residues (~20 t ha^{-1} fresh weight per year) derived from the olive trees and mulched *in loco* in late spring. Pruning residues had 51-55% total C (w/w; dry matter basis), 0.6-1.8% (w/w) total N, 0.4-1.2% (w/w) total K, and 0.4-1.2% (w/w) total P. The S_{IRR} treatment also included the use of cover crops mix of leguminous and cereal (*Avena sativa*) (5:1) sowed (180 kg ha^{-1}) in winter (December) of 2013, 2014, and 2015. The leguminous species were *Vicia sativa*, *Pisum sativum* subsp. *arvense*, *Trifolium alexandrinum*, *Vicia faba* var. *minor*, and *Medicago sativa*. In the subsequent spring, cover crops were mulched *in loco* (without being incorporated into the soil), supplying approx. 0.8 t ha^{-1} C.

The conventional block (C_{IRR}) served as a control treatment and was managed according to locally conventional soil management practices. The soil was tilled 2-3 times a year, herbicide was used (glyphosate, 1-2 times per year), and no organic material was supplied. Pruning residues (approx. 20 t ha^{-1} fresh weight) were removed each year and burnt outside the field. Chemical fertilizers were applied (centrifugal fertilizer spreader) at a rate of 300 kg ha^{-1} (0-0-50, N-P-K) and 300 kg ha^{-1} (21-0-0). Soil had similar characteristics at both C_{IRR} and S_{IRR} and it was a sandy-loam soil, pH 7.2, 0.67% OM, 55% sand, 26% silt and 18.7 clay. The RAW_{LLim} (10.7%dw) was estimated assuming 1.58 t m^{-3} BD as per the IT site. At the harvest time, the yield of 10 trees per treatment was measured (FW), averaged and reported as t ha^{-1}.

2.2 Soil CO2 efflux (Rs) measurements

<u>Rainfed, IT site:</u> Emissions of CO_2 from soil (R_s) were measured during 2015 using a portable infrared gas analyser (Li-6400, LI-COR, Lincoln, NE, USA) equipped with a soil respiration chamber (Model Li-6400-09) using a similar procedure adopted in Montanaro et al., (2012). Briefly, R_s was measured on average every approx. three weeks from January to

December within two hours during the central part of the day (12 – 14 h) at 30 locations per treatment distributed around three trees per treatment at 0.5, 1.0, 2.0, 3.5 m from row to inter-row accounting for the spatial variability of emissions (Almagro et al., 2009). At the same time as the R_s measurement, soil temperature (15 cm depth) was measured a few centimeters away using the 6000-09TC Li-COR temperature probe. Concurrently to R_s measurements, three soil bulk samples (from row to inter-row) were collected (0-35 cm depth) for soil moisture determinations (%dw, gravimetric method).

Irrigated, GR site: Emission of soil CO_2 and soil temperature were measured using the same model of the portable analyser used at the Italian site. Measurements were carried out from January to December 2015 in a mean time interval of approx. 4 weeks. On each occasion, measurements lasted within two hours during the central part of the day (12 – 14 h). At the beginning of the year, eight PVC collars were installed from row to inter-row as per the IT site. At each R_s sampling time, 24 locations per treatment distributed around three trees per treatment were measured. Concurrently, three soil bulk samples were collected (0-35 cm depth) from the row to inter-row for soil moisture determinations (%dw). Each sample included sub-samples collected at at 0 m, 0.4 m, 0.7 and 2.0 m from the row.

2.3 Data processing and analysis

The statistical analysis and data processing were performed using R software (4.1.2 version), plotting was done by OriginPro 9.3 (OriginLab Corporation, USA). Data were reported as the mean and standard error of the mean (±SE). The Student's *t*-test was used to examine the differences between treatments at each sampling date; the p values <0.05 were considered significant.

To account for the differential impact of soil temperature and moisture on the seasonal R_s, a conditional model was built embedding three sub-models (Y_1, Y_2, Y_3). In each sub-model, the flux of the CO_2 from soil (μmol m^{-2} s^{-1}) was the response variable (Y_n) of soil temperature and moisture based on the following conditions:

Y_1, if soil temperature < max_T and soil moisture >= RAW_{LLim};

Y_2, if soil temperature > max_T and soil moisture < RAW_{LLim};

Y_3, if soil temperature > max_T and soil moisture >= RAW_{LLim}.

The max_T was the soil temperature corresponding to the maximum R_s and was calculated as the μ value of the Gaussian distribution fitted to the pooled irrigated and rainfed R_s data under no soil moisture limitations, according to Richardson et al., (2012) and Yu et al., (2020). The values of the RAW_{LLim} were considered as splitting nodes and the R_s modelled through a Gompertz function, according to Yu et al., (2020).

All annual paired soil temperature, moisture, and R_s data from irrigated and rainfed sites were pooled in a single dataset (n =1476 records). The dataset was randomly split into validation (20%) and training (80%) fractions according to Roshan (2022) and a repeated random subsampling cross-validation procedure was applied.

The training dataset was partitioned based on the above-mentioned conditions to develop each pertaining sub-model (Y_1, Y_2, Y_3). Each training subset was repeatedly (k=10) subsampled (80%) at random with replacement generating k sub-train datasets. The excluded 20% of each k subsample was stored as the corresponding testing subset. Data from each K sub-train dataset were iteratively fitted and equations were parametrized, minimizing the squared residuals (measured values – fitted values). Then each k fitted sub-model was tested against the corresponding test subset and k mean absolute errors (MAE) between predicted and actual emissions values were calculated. Finally, the parameters belonging to the fitted sub-model with the lowest MAE were retrieved for the parametrization of each sub-model.

The parametrized Y_1, Y_2 and Y_3 sub-models were simultaneously integrated into the conditional model which was then validated using the validation dataset for each treatment/site combination (i.e., C_{IRR}, S_{IRR}, C_{RAIN}, S_{RAIN}). Subsequently, the Spearman's coefficient of correlation between predicted and actual values was determined.

3. Results

Data were sourced from experiments carried out at comparable olive groves located in two countries (Greece, Italy) with water supply (irrigation, rainfed) as the main difference between them. At both irrigated and rainfed sites, alternative management options (sustainable, conventional) differing in carbon retention practices were also employed. At the rainfed site, the mean (±SE) yield was 9.1±0.9 and 6.04±0.8 t ha^{-1} (FW) in the sustainable and conventional plots, respectively. At the irrigated site, the yield was 9.5±1.1 (sustainable) and 6.41±0.3 t ha^{-1} (conventional).

The resulting seasonal patterns of the R_s showed several consistencies, allowing its partitioning into three common main phases at both sites.

3.1 The seasonal trend of R_s, soil moisture and temperature

The seasonal variations of soil temperature and moisture and the related impact on R_s allow the partitioning of the seasonal emissions into three phases (Fig. 1 and 2): Phase I ranges from DOY (Day of Year) 20 to DOY 118 (rainfed site) and from 20 to 103 DOY (irrigated); Phase II included 142÷257 DOY range (rainfed) and 141÷257 DOY range (irrigated); Phase III included 286÷350 DOY range (rainfed) and 291÷357 DOY range (irrigated).

During Phase I, soil moisture was above RAW and values of R_s steeply increased during the early 15-17 weeks of the year in both countries. At the rainfed site, R_s increased from about 1 up to 4.1 ±0.19 (S_{RAIN}) and to 3.5 ±0.21 (C_{RAIN}) μmol CO_2 m^{-2} s^{-1} (Fig. 1A). At the irrigated site, the initial value of R_s was about 4.5 μmol CO_2 m^{-2} s^{-1} and was not dependent on treatments, then it picked at 7.2 ±0.39 μmol CO_2 m^{-2} s^{-1} (S_{IRR}) and 5.6 ±0.22 μmol CO_2 m^{-2} s^{-1} (C_{IRR} plot) (Fig. 2). After the R_s peak was reached, soil respiration entered the Phase II similarly in rainfed and irrigated sites (about 140 DOY), starting to decline towards the lowest seasonal level (Fig. 1A, 2A). Later in the season (DOI >250, Phase III), the R_s at both irrigated and rainfed sites increased to values similar to those of Phase I at about DOY 290; thereafter, it gradually reduced with the lowering of soil temperature to its minimum towards winter-time (Fig. 1A, B and Fig. 2A, B). On the whole-season basis, the mean R_s rate at the rainfed site was not significantly different between treatments, being 2.17 ±0.056 (SE) at C_{RAIN} and 2.32 ±0.06 μmol m^{-2} s^{-1} at S_{RAIN} plot. While that rate at the irrigated site was significantly (Student's *t*-test, α =0.05) influenced by management options being about 3.64±0.11 (C_{IRR}) and 4.05 ±0.15 μmol CO_2 m^{-2} s^{-1} (S_{IRR}), respectively.

The seasonal soil moisture ranged from about 7% to 20%dw (rainfed) and from about 14% to 27%dw (irrigated). From DOY 103 (irrigated) and DOY 118 (rainfed), onward soil moisture soon reached the lowest level of the season. The irrigation supplied at the GR site ensured the minimum mean soil moisture level at about 14%dw in both S_{IRR} and C_{IRR} treatments (Fig. 2B) whereas at the rainfed site soil moisture declined to about 7%dw in both C_{RAIN} and S_{RAIN} plots (Fig. 1B) till DOY 257 if a transient increase at DOY 226 is excepted (Fig. 1B). Soil temperature showed a similar seasonal pattern at both sites, starting from about 7°C (rainfed, IT) and about 15°C (irrigated, GR) reaching peak values of about

32°C in midsummer (Fig. 1B, 2B). Thereafter, soil temperature progressively declined to values similar to those recorded at the beginning of the year.

3.2 The R_s predicting model

The differential modulation of R_s caused by soil temperature and moisture across the various treatments and sites was integrated into a non-linear conditional model using soil temperature and moisture as both driving factors and decision nodes (Fig. 3).

The model was trained using various subsets of the training dataset defined according to the thresholds of soil temperature (max_T), which was 19.38 °C in this study (Fig. 4). Hence, max_T discriminated the R_s as a response variable of the exponential function of soil temperature (Y_1, Table 1) when soil temperature was <= max_T. When soil temperature was > max_T, R_s was modelled as response to (*i*) soil moisture when it was < RAW_{LLim} (Y_2, Table 1) and (*ii*) soil temperature (declining exp. function) when it was >= RAW_{LLim} (Y_3, Table 1). The conditional model integrating the three sub-models was then validated using the test fraction (20%) of the whole dataset not included in the training procedure. The values of measured and modelled soil respiration were in agreement across the various water supply (irrigated, rainfed) and management (conventional, sustainable) options showing a Spearman's coefficient of correlation test ranging from 0.67 to 0.96 (Fig. 4 and 5).

4. Discussion

This study shows the seasonal variation of soil CO_2 emissions in traditional olive ecosystems and identifies the stages when soil moisture and temperature are likely (and differentially) more influential on R_s because of their conceivable effect on autotrophic and heterotrophic processes and on the diffusivity of CO_2 within the soil (Tang et al., 2005; Xu and Shang, 2016; Hernández-Montes et al., 2017). The differential response of R_s to soil moisture and temperature was consistent across locations and management options and has been embedded in a predicting model.

4.1 Effect of management options on seasonal R_s

The soil CO_2 emission fluxes varied with the time of season and responded to the imposed treatments (*S*, *C*) to a different extent depending on the level of the main environmental drivers (i.e., soil temperature and moisture). The mean annual R_s rate at the rainfed was in line with that reported for comparable olive groves (Almagro et al., 2009).

At both sites, sustainable plots showed high R_s in most of the sampling dates compared to conventional (tilled). This would not agree with the impact of tillage on R_s. However, the instant instant peak in R_s in a tilled soil (5-15 cm depth) would last for a relatively short period (5-24 h) (Reicosky 1997; Al-Kaisi and Yin 2005). Hence, such a transient peak of R_s would not have been relevant. The generally higher R_s recorded at the *S* plots, were likely due to increased root and microbial activity (and population) (Lehmann 2003, Bechara et al., 2018). In addition, the high supply of carbon at the S plots will likely be due to high carbon substrate availability supporting additional microbial growth and in turn, an increase in microbial respiration (Rastogi et al., 2002, Davidson and Janssens, 2006).

The high soil CO_2 emissions recorded under carbon retention (sustainable) management might be environmentally criticizable. However, the impact of sustainable management should be apprised within an overall carbon balance accounting for removals and sequestrations of atmospheric CO_2 into various C pools of the ecosystem. For example, in a Mediterranean peach orchard, the sustainable management had a ~ 10% higher annual R_s compared to conventional one but an overall 48% higher net ecosystem productivity (Montanaro et al., 2017b). In addition, the approx. 50% increased yield achieved at the C plots compared to S ones is in line with the effect of improved carbon retention practices as shown in a metanalysis carried out on Mediterranean tree crops including olive groves (Morugán-Coronado et al., 2020).

Notably, at the beginning of the season, soil temperature differed between IT and GR olive groves by about 8-10 °C (Fig. 1B and 2B) likely due to the different geographical locations. This would also explain the different value of R_s between the two sites detected at the beginning of the season. The steep increase of the R_s recorded during the Phase I is comparable with those recorded in similar olive ecosystems (Almagro et al., 2009; Chamizo et al., 2017).

As expected, the different water supply induced different soil moisture patterns between sites, remaining within RAW (irrigated) or declining below RAW_{LLim} (rainfed). In addition, at the rainfed site, soil moisture at S_{RAIN} plot had a slow decline plausibly due to the high deep soil water holding capacity due to the high OM concentration (1.29% C_{RAIN} *vs* 1.67% S_{RAIN}, see M&M section) (Celano et al., 2011). The high soil moisture and OM might have sustained a high photosynthetic activity of the tree and likely contributed to modulate soil respiration (Tang et al., 2005) supporting the significantly higher R_s recorded during Phase II in S_{RAIN} plot compared to C_{RAIN} one (Fig. 1A).

The decline of the R_s detected at irrigated and rainfed sites during Phase II, despite soil temperature increasing (Fig. 1, 2) is consistent with reports on other perennial ecosystems including olive, peach and citrus (Almagro et al., 2009; Montanaro et al., 2012; Munjonji et al., 2021). However, the underlying mechanisms would differ between sites (see below the "*Bimodal effect*" paragraph). Later in the season (DOI >250, Phase III), the overall plant physiology conceivably recovered from summer environmental limitations (e.g., drought, high irradiance) similarly to R_s data measured in other perennials mentioned above.

Under irrigation, soil moisture would have values ranging between field capacity (FC) and a threshold value established by the irrigation manager. Under rainfed Mediterranean conditions, soil moisture usually ranges from field capacity (FC) to low values approaching the wilting point (WP) (Fig. 1).

The present study was carried out in the real world, collecting the variability of soil moisture occurring under rainfed and drip irrigation. Drip irrigation was set preventing soil moisture values to fall below the RAW. This approach allowed to collect of R_s data within as wide as possible moisture range (from FC to WP). Different irrigation regimes having different threshold criteria including PRD, RDI, etc., would induce a change in soil moisture dynamics, but moisture values would fall in the range recorded across the various Phases and sites of the present study. The irrigation regime per se does not impact R_s, while the soil moisture resulting upon an irrigation regime would be. However, in future work it would be of interest to test the model developed in groves under different irrigation regimes characterizing their impact on R_s.

4.2 Bimodal effect of soil temperature and moisture on R_s

The positive dependence of R_s on soil temperature is widely reported and an exponential equation usually explains their relationship. However, within a range of temperature, the maximum R_s occurs at a threshold soil temperature depending on the level of co-occurring factors including SOC, microbial biomass and soil moisture (Richardson et al., 2012). Hence, increasing temperature above that optimum does not increase the release of CO_2, but indeed R_s would be constrained by limiting factors such as substrate availability, microbial populations, and moisture (Giardina and Ryan, 2000; Richardson et al., 2012; Davidson and Janssens, 2016).

In addition, soil moisture and temperature might reciprocally mask their effect on R_s. To solve this complexity, Almagro et al., (2009) proposed a month-based partition of the season in “growing” (October-April) and “dry” (May-September) seasons. Here, we propose to mechanistically identify soil temperature and moisture values to be used as thresholds delineating stages when these factors differentially act as prominent drivers of R_s.

In this study, throughout the annual cycle, the soil temperature ranged from about 4°C to about 36°C when soil moisture oscillated within RAW (i.e., >= ~11%dw) and up to 45°C when moisture oscillated below RAW (i.e., < ~11%dw). Pooling all R_s data recorded across the experimental sites under no soil moisture limitations (i.e., > RAW_{LLim}) revealed a differential response of R_s to temperature and that the maximum R_s occurred at about 20°C (namely 19.38°C, Fig. 6). Emissions of CO_2 occurring when soil temperature was below the max_T one (left, Fig. 6) corresponded to those of Phase I and III, when temperature drove the R_s, confirming their close relationship (González-Real et al., 2018) (Fig. 7).

Emissions occurring at soil temperature above max_T in Figure 6 were substantially those from the irrigated site where soil moisture was non-limiting (see Fig. 1A and 2A). Under these conditions, the release of CO_2 was not influenced by soil moisture (Fig. 8A) but it was somehow sensitive to soil temperature, showing a declining pattern with increasing temperature (Fig. 8B). This finding confirms that the soil temperature of about 20°C was the "optimal" one, i.e. causing the highest R_s *in sensu* Richardson et al., (2012),

A similar soil temperature threshold might be inferred from a study carried out at a comparable traditional irrigated olive grove (Chamizo *et al*., 2017), showing the decline of R_s occurring when the temperature was > max_T even though soil water content (SWC) was stable at about 20%vol (i.e., approx. 14.2%dw assuming 1.4 bulk density). A negative correlation between R_s and temperature >20°C under good irrigation (moisture >20%vol) also appears for high density olive groves (Testi et al., 2008). Hence, the soil temperature threshold approach proposed in this paper would apply to various olive ecosystems. However, it remains to be specifically tested.

The declining pattern of R_s in response to increasing soil temperature contrasts with the general positive exponential effect of soil temperature on R_s. However, in a meta-analysis study across nine biomes (and 27 papers), such an exponential relationship has been criticized, showing that R_s increases with soil temperature up to ~25 °C and that rising temperatures above that threshold decrease R_s (Carey et al., 2016). Such a temperature-dependent limitation of R_s might effectively be due to the indirect effect of temperature, such as the putative scarcity of substrate availability and of microorganisms capable of respiring at these temperatures (Giardina and Ryan, 2000). In addition, considering that the high air vapour pressure deficit (*VPD*) and temperature occurring during summer, even for well-irrigated plants, would induce a diffusional limitation of photosynthesis (low mesophyll conductance) (Fernández 2014), possibly the environmental conditions (i.e., *VPD*) during Phase II might have limited photosynthetic activity and in turn R_s (Tang et al., 2005). However, the causes of high temperature-induced limitation of R_s when soil moisture falls within RAW remain to be elucidated.

Soil moisture influences R_s at both low (inhibiting microbial activity) and high levels (reducing aerobic decomposition and within-soil gas diffusion processes) (Subke et al., 2003). An additional mechanism linking soil moisture and R_s is based on the evidence that soil moisture influences plant physiological activity (e.g., photosynthesis), which might regulate the autotropic component of R_s, as discussed above.

The moisture dependence of R_s occurring when moisture is a limiting factor might dominate upon temperature dependence as shown, for example, in a *Quercus spp.* forest (Rey et al., 2002). Accordingly, at the rainfed site, when soil moisture fell below RAW_{LLim},

CO_2 emissions did not show any correlative pattern with temperature (Fig. 9A), while R_s positively responded to soil moisture increase (Fig. 9B) following a growing Gompertz function and achieving an asymptotic value when moisture approached the RAW_{LLim}.

The sigmoidal pattern of R_s as a response to even a minimal increase of soil moisture, observed at the rainfed site, agrees with that reported by Subke et al. (2003) and Yu et al. (2020). Hence, under low soil moisture conditions, the lower threshold of RAW might be a switch value identifying the time of the season when soil CO_2 emission is less sensitive to soil temperature and becomes limited by soil moisture. In the present study, a complete separation of the soil temperature effect from that of moisture was not pursued. This separation would provide more insights in the mechanisms regulating R_s via an independent manipulation of them under laboratory conditions (e.g., Conant et al., 2004) or even under open field conditions (e.g., Zhong et al., 2016). However, the present paper identified the threshold values of moisture and soil tempertuure distinguishing those stages when they are the prominent limiting or activating factor of R_s.

4.3 Modelling the influence of temperature and moisture on Rs

The use of algorithms, e.g., Random Forests (RF) for classification and regression problems is increasingly used, particulalrly for massive dataset having a large number of predictors even greater than observations (Efron, 2020; Schonlau and Zou, 2020). Our conditional model resemble a RF model with two predictors, however they differ in the principle of splitting nodes. In RF model, predictors and data are selected at random while in our conditional model there is a rationale on which the predictors (moisture and temperatore) are used as splitting nodes and independent variable of functions targeting R_s.

Nowadays, there is a growing need to provide reliable (and affordable) estimations of carbon fluxes (including R_s) occurring in agricultural ecosystems to quantify, for example, their mitigation potential (Kuhnert et al., 2017). Soil respiration is a relevant component of the carbon cycle, sharing up to 85-90% of the C cycle (Xu and Shang, 2016), making its estimation essential to increase knowledge on the interaction between agroecosystems and the environment (e.g., Plénet et al. 2022).

Specifically, traditional olive tree crops, due to their long lifespan and C sequestration capability, are recognized as relevant tree crops for climate change mitigation purposes, deserving attention within the *Product Environmental Footprint* launched by the European Commission to define indicators of the environmental performance of agri-food products (EC, 2013). In this context, affordable and reliable procedures for estimating R_s might be of assistance when implementing environmental labelling of food products (Hélias et al., 2022). There are various models including soil temperature and moisture developed to estimate the release of CO_2 from soil at agricultural crops (e.g., Almagro et al., 2009; Chen et al., 2011). However, to the best of our knowledge, this paper offers a new approach for predicting the R_s based on the occurrence of those drivers under specific conditions, showing that the resulting conditional model was able (*i*) to collect the seasonal oscillations of R_s consistently with the time frame of the various Phases identified (Fig. 4 and 5) and (*ii*) to explain about 84% of the variance of R_s (Fig. 10). The accuracy of the model, as measured through the R^2, confirms the prominent role of soil temperature and moisture on R_s and that additional variables have to be influential on R_s (Xu and Shang, 2016).

Particularly, in olive ecosystems an inter-annual variability in R_s could be expected due the variable plant physiological activities related to variable yield as consequence of the “on” and “off” year typical for Mediterranean traditional olive systems. Inter.annual variability would have an impact on R_s greater than the responses to warming as recently documented in an alpine meadow (Fu and Shen, 2022). In this study, the R_s model was trained and parametrized on a dataset encompassing the data of both countries, hence ensuring the higher range of soil conditions (soil temperature, moisture) and R_s. The approach of parametrizing a model on a wide range of conditions would be in favour of its broad application as discussed, for example, by Saxton and Rawls (2006) who modelled soil water characteristics estimating model parameters in the full range of soil moisture.

5. Conclusions

The soil CO_2 emissions data were gathered at traditional olive ecosystems under different water supply (rainfed, irrigation) and management options (sustainable, conventional), revealing a consistent phase-based partitioning of the annual R_s across treatments and sites. Hence, the rationale of the phase-based approach proposed in this paper would be generalizable.

Under carbon retention (sustainable) management, soil CO_2 emissions were high in some periods of the annual cycle, which might be environmentally criticizable. However, the impact of sustainable management should be apprised within an overall carbon balance accounting for removals and sequestrations of atmospheric CO_2 into various C pools of the ecosystem.

In this study, the response of R_s to soil temperature and moisture has been parameterized in relation to soil moisture (i.e., lower limit of RAW) and temperature (i.e., max_T corresponding to maximum R_s). These factors served as effective predictors and splitting nodes of a simple and efficient conditional model capable of explaining about 84% of the total annual variance of R_s. This paper describes the impact of the environment-management interaction on the release of CO_2 from soil. Results would support carbon accounting procedures tailored to estimating the sink/source capability of traditional olive ecosystems within environmental-friendly agricultural domains.

CRediT authorship contribution statement

G.M and G.K conceived the study; G.M, G.D., N. Kavroulakis, E. M., performed the field work and the laboratory analyses; G.M. analysed the data and wrote the original draft of the manuscript; N. Kourgialas, G.P., G.K, B.D., V.N. reviewed and edited the manuscript, all authors gave final approval for publication.

Declaration of Competing Interest

The authors declare that they have no known competing financial interests or personal relationships that could have appeared to influence the work reported in this paper.

Funding

The study was partially funded by the 2014–2020 Rural Development Programme for Basilicata Region (Misura 16.1, Inno_Olivo&Olio, CUP C31B18000590002). With the contribution of the LIFE+ financial instrument of the European Union for the project LIFE11 ENV/GR/942 /oLIVECLIMA.

Acknowledgements

GM thanks F. Montanaro for advices on conditional models.

References

Al-Kaisi, M., Yin, X., 2005. Tillage and crop residue effects on soil carbon and carbon dioxide emissions in corn-soybean rotations. J. Environ. Qual. 34, 437-445.

Arampatzis, G., Hatzigiannakis, E., Pisinaras, V., Kourgialas, N., Psarras, G., Kinigopoulou, V., Panagopoulos, A., Koubouris, G., 2018. Soil water content and olive tree yield responses to soil management, irrigation, and precipitation in a hilly Mediterranean area. J. Water Clim. Change 9, 672–678.

Bechara, E., Papafilippaki, A., Doupis, G., Sofo, A., Koubouris, G., 2018. Nutrient dynamics, soil properties and microbiological aspects in an irrigated olive orchard managed with five different management systems involving soil tillage, cover crops and compost. J. Water Clim. Change 9, 736–747.

Bhogal, A., Nicholson, F.A., Chambers, B.J., 2009. Organic carbon additions: effects on soil bio-physical and physico-chemical properties. European J. Soil Sci. 60, 276–286.

Carey, J.C., Tang, J., Templer, P.H., Kroeger, K.D., Crowther, T.W. et al., 2016. Temperature response of soil respiration largely unaltered with experimental warming. Proceedings of the National Academy of Sciences 113, 13797–13802. https://doi.org/10.1073/pnas.1605365113

Celano, G., Palese, A.M., Ciucci, A., Martorella, E., Vignozzi, N., Xiloyannis, C., 2011. Evaluation of soil water content in tilled and cover-cropped olive orchards by the geoelectrical technique. Geoderma 163, 163–170. https://doi.org/10.1016/j.geoderma.2011.03.012

Chen, X., Post, W.M., Norby, R.J., Classen, A.T., 2011. Modeling soil respiration and variations in source components using a multi-factor global climate change experiment. Climatic Change 107(3), 459–80. https://doi.org/10.1007/s10584-010-9942-2.

Conant, R. T., Dalla-Betta, P., Klopatek, C. C., & Klopatek, J. M., 2004. Controls on soil respiration in semiarid soils. Soil Biology and Biochemistry, 36(6), 945-951.

Davidson, E.A., Janssens, I.A., 2006. Temperature sensitivity of soil carbon decomposition and feedbacks to climate change. Nature 440, 165–173. https://doi.org/10.1038/nature04514

EC., 2013. European Commission. Commission Recommendation of 9 April 2013 on the Use of Common Methods to Measure and Communicate the Life Cycle Environmental Performance of Products and Organisations. Off. J. Eur. Union 2013, L124, 1–210.

Efron, 2020. Prediction, Estimation, and Attribution. Journal of The American Statistical Association, 115(530): 636–655.

Eggleston, H.S., Buendia, L., Miwa, K., Ngara, T., Tanabe, K. IPCC Guidelines for National Greenhouse Gas Inventories; ICCP: Ridderkerk, The Netherlands, 2006.

FAO, 2022. Food and agriculture data. License: CC BY-NC-SA 3.0 IGO. Extracted from: https://www.fao.org/faostat/en/#data. Data of Access: 20-05-2022.

Fernández J.E., 2014. Understanding olive adaptation to abiotic stresses as a tool to increase crop performance. Environmental and Experimental Botany, 103: 158-179, https://doi.org/10.1016/j.envexpbot.2013.12.003.

Franzluebbers, K., Fanzluebbers, A.J., Jawson, M.D., 2002. Environmental controls on soil and whole-ecosystem respiration from a tallgrass prairie. Soil Sci. Soc. Am. J. 66, 254–262.

Fu, G., Shen, Z.-X., 2022. Asymmetrical warming of growing/non-growing season increases soil respiration during growing season in an alpine meadow. Science Total Env, 812: 152591, doi: 10.1016/j.scitotenv.2021.152591.

Giardina, C.P., Ryan, M.G., 2000. Evidence that decomposition rates of organic carbon in mineral soil do not vary with temperature. Nature 404, 858–861. https://doi.org/10.1038/35009076

González-Real, M.M., Martin-Gorriz, B., Egea, G., Nortes, P.A., Baille, A., 2018. Characterization and modelling of soil CO2 efflux in old and young irrigated citrus orchards. CATENA 162, 376–385. https://doi.org/10.1016/j.catena.2017.10.025

Hélias, A., van der Werf, H.M.G., Soler, LG. et al. 2022. Implementing environmental labelling of food products in France. Int J Life Cycle Assess 27, 926–931. https://doi.org/10.1007/s11367-022-02071-8

Hernández-Montes, E., Escalona, J.M., Tomás, M., Medrano, H., 2017. Influence of water availability and grapevine phenological stage on the spatial variation in soil respiration: Water status and vine phenology affect soil respiration. Australian

Journal of Grape and Wine Research 23, 273–279. https://doi.org/10.1111/ajgw.12279

Kavvadias V., Koubouris G. (2019) Sustainable Soil Management Practices in Olive Groves. In: Panpatte D., Jhala Y. (eds) Soil Fertility Management for Sustainable Development. Springer, Singapore. DOI: https://doi.org/10.1007/978-981-13-5904-0_8

Kavvadias V., Papadopoulou M., Vavoulidou E., Theocharopoulos S., Koubouris G., Psarras G., Manolaraki C., Giakoumaki G. & Vasiliadis A. (2018) Effect of sustainable management of olive tree residues on soil fertility in irrigated and rain-fed olive orchards. Journal of Water and Climate Change, 9 (4), doi: 10.2166/wcc.2018.143.

Koubouris, G.C., Kourgialas, N.N., Kavvadias, V., Digalaki, N., Psarras, G. (2017) Sustainable Agricultural Practices for Improving Soil Carbon and Nitrogen Content in Relation to Water Availability–An Adapted Approach to Mediterranean Olive Groves. Communications in Soil Science and Plant Analysis, 48 (22), pp. 2687-2700. doi: 10.5004/dwt.2017.21548

Kourgialas, N. N., Koubouris, G. C., Dokou, Z., 2019. Optimal irrigation planning for addressing current or future water scarcity in Mediterranean tree crops. Science of The Total Environment 654, 616–632.

Kourgialas, N.N., Doupis, G., Psarras, G., Sergentani, C., Digalaki, N., Koubouris, G.C., 2017. Soil management and compost effects on salinity and seasonal water storage in a Mediterranean drought-affected olive tree area. Desal. Water Treat. 99, 42–48

Kuhnert, M., Yeluripati, J., Smith, P., et al. 2017. Impact analysis of climate data aggregation at different spatial scales on simulated net primary productivity for croplands. European Journal of Agronomy, Uncertainty in crop model predictions 88, 41–52. https://doi.org/10.1016/j.eja.2016.06.005

Lehmann, J., 2003. Subsoil root activity in tree-based cropping systems. Plant Soil 255, 319–331.

Michalopoulos, G.; Kasapi, K.A.; Koubouris, G.; Psarras, G.; Arampatzis, G.; Hatzigiannakis, E.; Kavvadias, V.; Xiloyannis, C.; Montanaro, G.; Malliaraki, S.; Angelaki, A.; Manolaraki, C.; Giakoumaki, G.; Reppas, S.; Kourgialas, N.; Kokkinos, G. Adaptation of Mediterranean Olive Groves to Climate Change through Sustainable Cultivation Practices. *Climate* 2020, *8*, 54.

Montanaro G., Tuzio A.C., Xylogiannis E., Kolimenakis A., Dichio B., 2017b. Carbon budget in a Mediterranean peach orchard under different management practices.

Agriculture, Ecosystems and Environment, 238: 104-113, DOI: 10.1016/j.agee.2016.05.031

Montanaro G., Xiloyannis C., Nuzzo V., Dichio B., 2017a. Orchard management, soil organic carbon and ecosystem services in Mediterranean fruit tree crops. Scientia Horticulturae, 217: 92-101, DOI: 10.1016/j.scienta.2017.01.012

Montanaro, G., Nuzzo, V., Xiloyannis, C., Dichio B., 2018. Climate change mitigation and adaptation in agriculture: the case of the olive. Journal of Water and Climate Change, 9 (4): 633–642. doi: https://doi.org/10.2166/wcc.2018.023

Morugán-Coronado, A., Linares, C., Gómez-López, M.D., Faz, A., Zornoza, R., 2020. The impact of intercropping, tillage and fertilizer type on soil and crop yield in fruit orchards under Mediterranean conditions: A meta-analysis of field studies. Agricultural Systems, 178:102736, https://doi.org/10.1016/j.agsy.2019.102736.

Munjonji, L., Ayisi, K.K., Mafeo, T.P., Maphanga, T., Mabitsela, K.E., 2021. Seasonal variation in soil CO2 emission and leaf gas exchange of well-managed commercial Citrus sinensis (L.) orchards. Plant Soil 465, 65–81. https://doi.org/10.1007/s11104-021-04986-x

Palese, A.M., Pergola M., Favia M., Xiloyannis C., Celano G., 2013. A sustainable model for the management of olive orchards located in semi-arid marginal areas: Some remarks and indications for policy makers. Environmental Science & Policy, 27:81-90.

Plénet, D., Borg, J., Barra, Q., Bussi, C., Gomez, L., Memah, M.-M., Lescourret, F., Vercambre, G., 2022. Net primary production and carbon budget in peach orchards under conventional and low input management systems. European Journal of Agronomy 140, 126578. https://doi.org/10.1016/j.eja.2022.126578

Rallo, G., Baiamonte, G., Manzano, J.J., Povenzano, G., 2014. Improvement of FAO-56 Model to estimate transpiration flux of drought tolerent crops under soil water deficit: application for olive groves. Irrigation and drainage Engineering, ASCE, A4014001, 1-8. Doi: 10.1061/(ASCE)IR.1943-4774.0000693.

Rastogi, M., Singh, S., Pathak, H., 2002. Emission of carbon dioxide from soil. Current Sci. 82(5), 510-517.

Reicosky, D.C., 1997. Tillage-induced CO_2 emission from soil. Nutr. Cycl. Agroecosyst. 49, 273–285

Rey A, Pegoraro E, Tedeschi V, De Parri I, Jarvis PG, Valentini R. 2002. Annual variation in soil respiration and its components in a coppie oak forest in Central Italy. Glob Change Biol 8:851–66.

Richardson, J., Chatterjee, A., Jenerette, D., 2012. optimum temperatures for soil respiration along a semi-arid elevation gradient in southern california. Soil Biology and Biochemistry 46: 89–95. https://doi.org/10.1016/j.soilbio.2011.11.008.

Roshan, J.V. 2022. Optimal ratio for data splitting. Statistical Analysis and Data Mining: The ASA Data Science Journal 15, fasc. 4 (2022): 531–38. https://doi.org/10.1002/sam.11583.

Sanz-Cobena, A., Lassaletta, L., Garnier, J., Smith, P., 2017. Mitigation and quantification of greenhouse gas emissions in Mediterranean cropping systems. Agriculture, Ecosystems & Environment, 238: 1-4, https://doi.org/10.1016/j.agee.2016.12.032.

Saxton, K.E., Rawl, W. J., 2006. Soil water characteristic estimates by texture and organic matter for hydrologic solutions. Soil Sci. Soc. Am. J. 70:1569–1578. doi:10.2136/sssaj2005.0117

Schonlau, M., Zou, R. Y., 2020. The random forest algorithm for statistical learning. The Stata Journal, 20(1), 3-29.

Chamizo, S., Penélope Serrano-Ortiz, Ana López-Ballesteros, Enrique P. Sánchez-Cañete, José Luis Vicente-Vicente, Andrew S. Kowalski. 2017. Net ecosystem CO2 exchange in an irrigated olive orchard of SE Spain: Influence of weed cover. Agriculture, Ecosystems & Environment, Volume 239, Pages 51-64, https://doi.org/10.1016/j.agee.2017.01.016.

Tang, J., Baldocchi, D.D., Xu, L., 2005. Tree photosynthesis modulates soil respiration on a diurnal time scale. Global Change Biology 11, 1298–1304. https://doi.org/10.1111/j.1365-2486.2005.00978.x.

Testi, L., Orgaz, F., Villalobos, F., 2008. Carbon exchange and water use efficiency of a growing, irrigated olive orchard. Environmental and Experimental Botany 63, 168–177. https://doi.org/10.1016/j.envexpbot.2007.11.006

Wang,W.J., Dalal, R.C., Moody, P.W., Smith, C.J., 2003. Relationship of soil respiration to microbial biomass, substrate availability and clay content. Soil Biol. Biochem. 35, 273–284.

Xu, M., Shang, H., 2016. Contribution of soil respiration to the global carbon equation. Journal of Plant Physiology, Plants facing Changing Climate 203, 16–28. https://doi.org/10.1016/j.jplph.2016.08.007

Yu, H., Xu, Z., Zhou, G., Shi, Y., 2020. Soil carbon release responses to long-term versus short-term climatic warming in an arid ecosystem. Biogeosciences 17, 781–792. https://doi.org/10.5194/bg-17-781-2020

Zhong, Z.M., Shen, Z.X., Fu, G. 2016. Response of soil respiration to experimental warming in a highland barley of the Tibet. SpringerPlus 5, 137: https://doi.org/10.1186/s40064-016-1761-0

Tables

Table 1 - Equations and related parameters (±SE) of the sub-models integrated into the conditional model (Fig. 7) to estimate CO_2 soil emission (R_s) as a response variable (Y_n) of soil temperature (T) and soil water content (SWC).

Sub-model	Parameters	Comments
$Y_1 = a \times \exp^{b \times T}$	a= 0.4718±0.046*** b=0.1387±0.006***	Function describing R_s as response of soil temperature (T) in case of soil moisture within the Readily Available Water and T<20°C. Phase I and III in this study
$Y_2 = a \times \exp^{-\exp(b \times (SWC - xc))}$	a=2.84± 0.2272 *** b= 1.0587±0.55 "." xc= 6.1425±0.387***	Function describing R_s as response to SWC in case of soil moisture values are below Readily Available Water and T>20°C. Phase II, rainfed condition in this study.
$Y_3 = a \times (T - xc)^{-b}$	a=10.78±7.23, b= 0.6182±0.226** xc =16.379±2.354***	Function describing R_s as response to soil temperature in case of soil moisture values are within Readily Available Water and T>20°C. Phase II, irrigated condition in this study.

Significance codes: ***, α = 0.001; ** α=0.01, * α=0.05, "." α=0.1. Functions' parameters have been tuned through a repeated resampling cross-validation procedure.

Figure captions

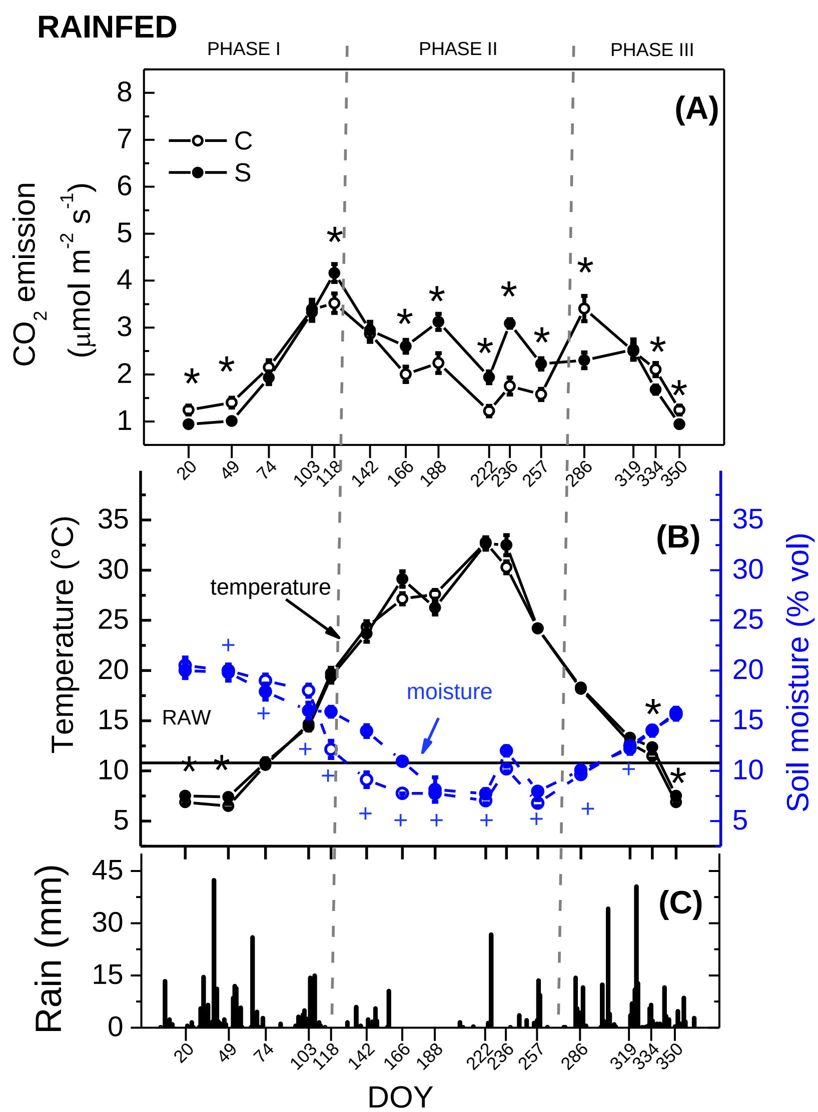

Fig. 1. Seasonal variation of (A) midday (12-14 h) CO_2 soil emissions, (B) soil temperature (continuous line) and moisture (dashed lines) and (C) rain at the olive orchards under (○) conventional and (●) sustainable management measured at the rainfed site. DOY= day of year. Each CO_2 emission and temperature point is the mean of 30 measurements (±SE); for soil moisture, each point is the mean of 3 bulk samples (±SE). The horizontal line appearing on panel (B) represents the level of soil moisture corresponding to the lower threshold of the readily available water (RAW). For each parameter, comparison of treatments at the same time * (temperature, CO_2 emissions) and + (soil moisture) indicate statistically significant differences (Student's *t*-test, $p<0.05$).

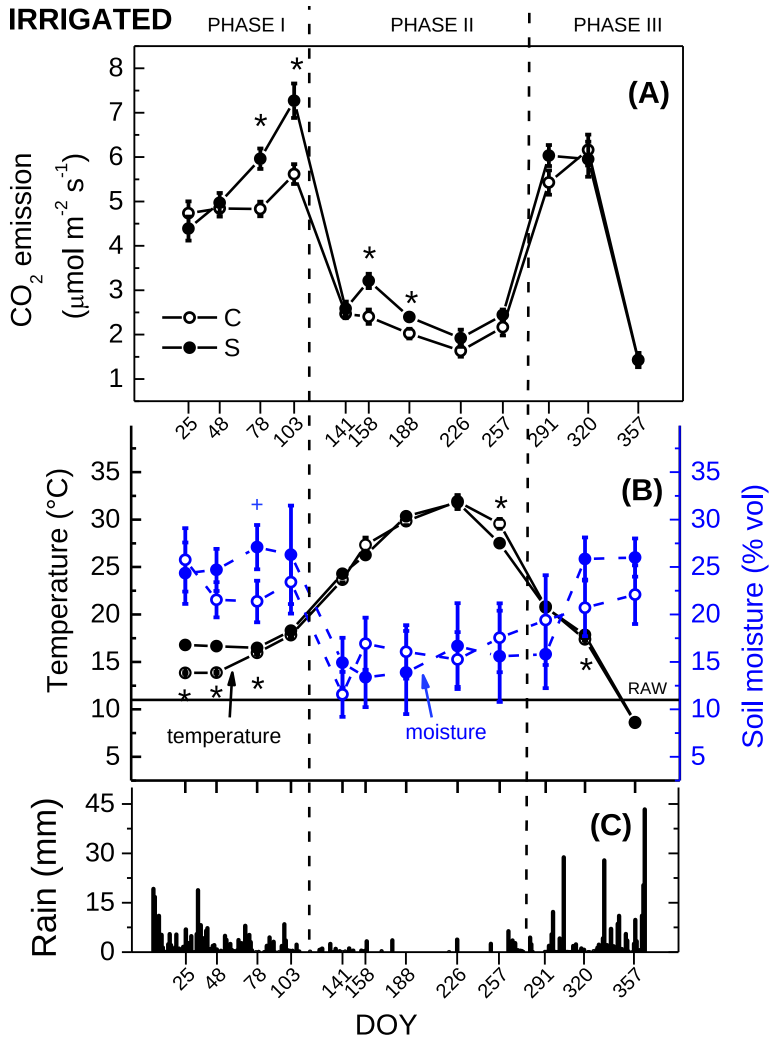

Fig. 2. Seasonal variation of (A) midday (12-14 h) CO_2 soil emissions, (B) soil temperature (continuous line) and moisture (dashed lines) and (C) rain at the olive orchards under (○) conventional and (●) sustainable management measured at the irrigated (GR) site. DOY= day of year. Each CO_2 emission and temperature point is the mean of 24 measurements (±SE); for soil moisture, each point is the mean of 3 bulk samples (±SE). The horizontal line appearing on panels (B) represents the level of soil moisture corresponding to the lower threshold of the readily available water (RAW). For each parameter, comparison of treatments at the same time * (temperature, CO_2 emissions) and + (soil moisture) indicate statistically significant differences (Student's *t*-test, $p<0.05$).

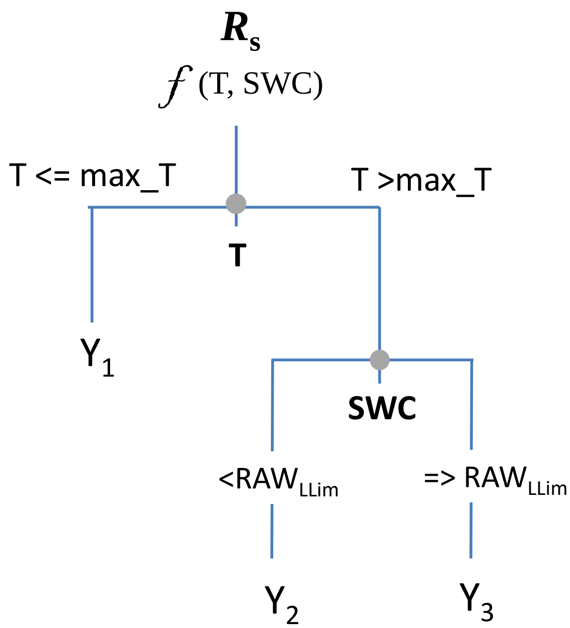

Fig. 3. Schematic of the decision tree of the model to predict soil respiration (R_s) as response variable Y_n of soil temperature (T) and soil water content (SWC) which also act as conditional split points of the model. The threshold temperature (max_T) was set at 19.38 °C; the threshold values of SWC were based on the lower limit of the readily available water (RAW_{LLim}) which was 10.7%dw. For details on each Y_n equation, please refer to Table 1.

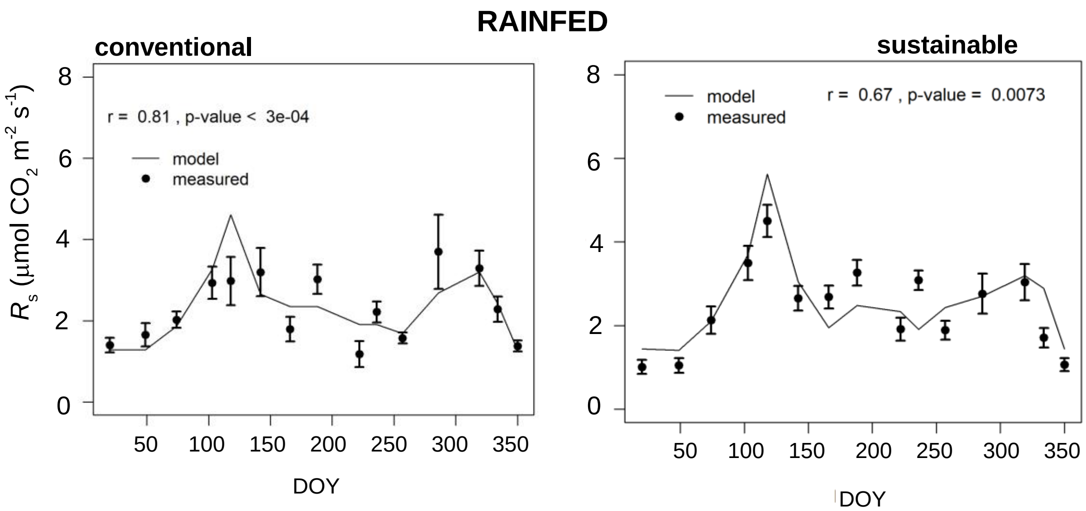

Fig. 4. Seasonal trend of the predicted (−) and the measured soil respiration (R_s) (•, ±SE) at the rainfed site under conventional (left) and sustainable (right) management conditions. The values of the correlation test (r) and *p*-value refer to the Spearman's rank test carried out on paired measured-predicted R_s values. DOY= day of year.

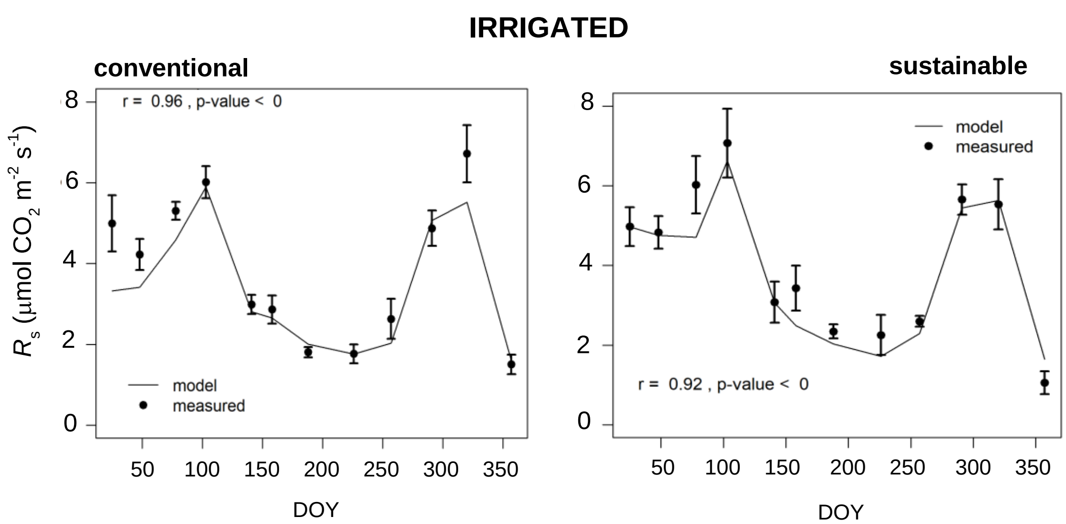

Fig. 5. Seasonal trend of the predicted (−) and the measured soil respiration (R_s) (•, ±SE) at the irrigated site under conventional (left) and sustainable (right) management conditions. The values of the correlation test (r) and *p*-value refer to the Spearman's rank test carried out on paired measured-predicted R_s values. DOY= day of year.

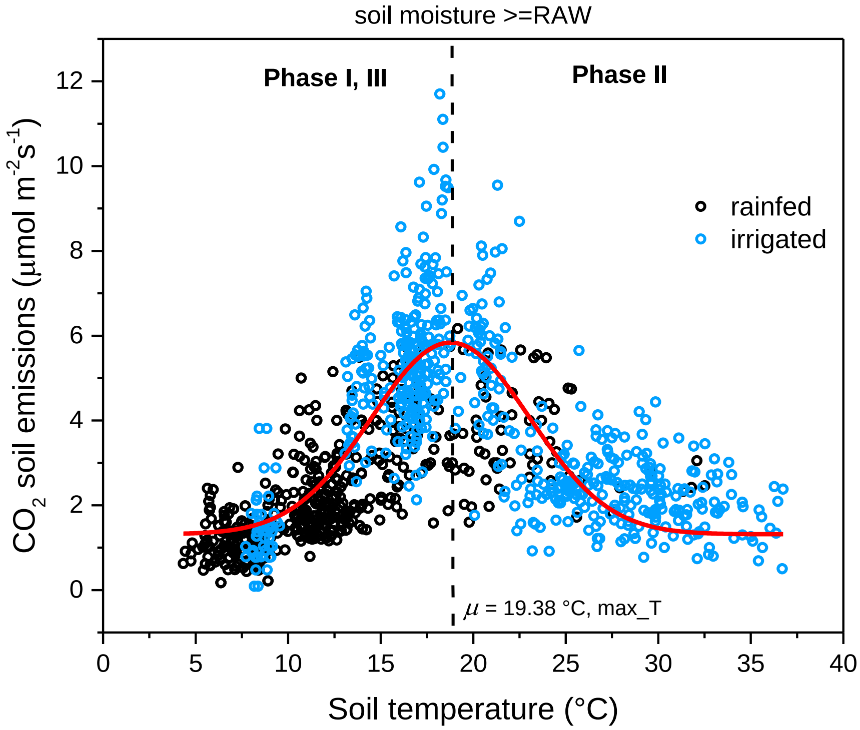

Fig. 6. Correlation between the whole annual soil respiration (R_s) and soil temperature recorded at both irrigated and rainfed sites under non-limiting soil moisture conditions. The vertical dashed line indicates the centre μ of the fitting Gaussian curve which represents the max_T. The Phases I, II and III refer to those of Fig. 1 and 2.

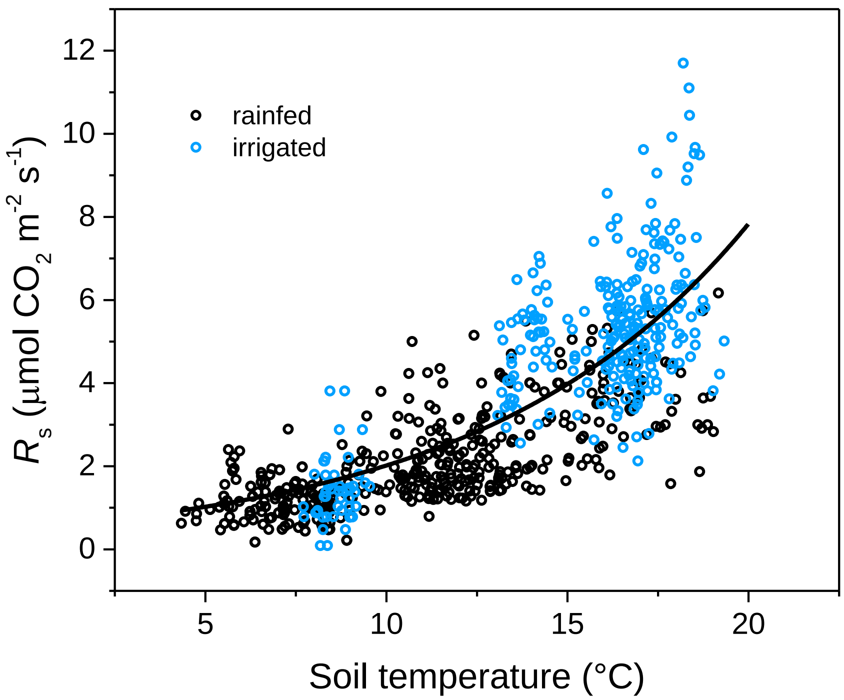

Fig. 7. Correlation between soil temperature and CO_2 soil emissions (R_s) recorded under no soil moisture limitation (i.e., >= RAW_{LLim}) during Phase I and III at both irrigated and rainfed sites. Data from the two sites have been pooled before fitting; note that the fitting line is illustrative only, please for model's details refer to Table 1.

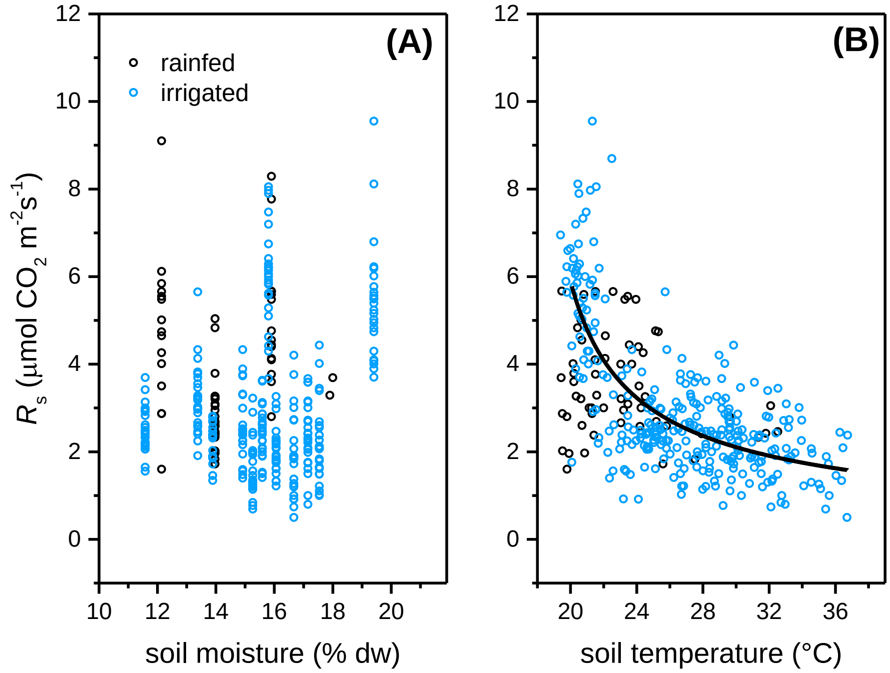

Fig. 8. Correlation between soil CO_2 emissions (R_s) and (A) soil moisture and (B) soil temperature measured during the Phase II at irrigated (GR) and rainfed (IT) sites under moisture within the readily available water. Data from the two sites have been pooled before fitting; note that the fitting line is illustrative only, please for model's details refer to Table 1.

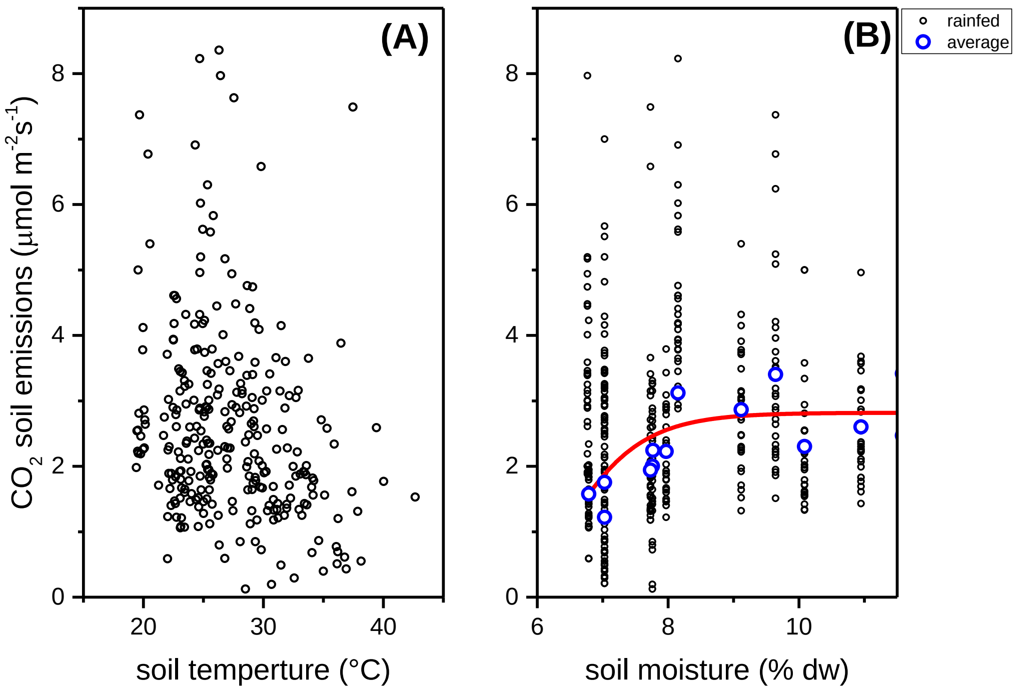

Fig. 9. Correlation between soil CO_2 emissions and (A) soil temperature and (B) soil moisture. Data refer to those collected under moisture limitation, hence, any data from the irrigated site appears. For details on the Gompertz fitting function (panel B), please refer to Table 1.

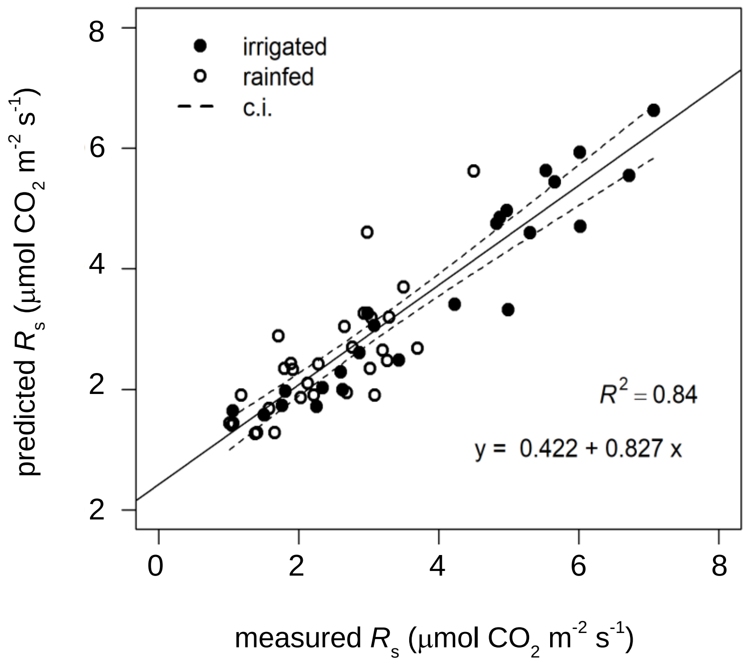

Fig. 10. Correlation between the measured and predicted mean soil respiration (R_s) using the conditional model (Fig. 7, Tab. 1). Dashed lines represent the 95% c.i. Data from irrigated and rainfed sites have been pooled before fitting. Each point is the mean of 5-6 values.